Romanian Reports in Physics, Vol. 60, No. 4, P. 1053–1063, 2008

AUTOMATED OPTOELECTRONIC DEVICE FOR QUALITATIVE ANALYSIS OF THE ARTWORK SURFACES USING THE LIF TECHNIQUE

L. ANGHELUTA, J. STRIBER, R. RADVAN, M. SIMILEANU

National Institute of Research and Development for Optoelectronics – INOE 2000, CERTO
1 Atomistilor Street, Magurele – Ilfov, Romania, e-mail: laurentiu@inoe.inoe.ro

(Received April 7, 2008)

Abstract. The aim of this paper is to describe the construction of an automated scanning device that uses the LIF invesitgation method, and to verify its operation and efficiency in the particular study case of an historical parchment.

Keywords: LIF Scanning, automated scanning device, fluorescence.

1. INTRODUCTION

In the decades that followed the discovery of the laser effect, there were made a lot of studies in the field of laser interaction with the matter. Among the most important uses of it there can be found the most novel investigation and analysis techniques of the surfaces that interacts with the laser radiation.

Two of these investigation techniques that are using the laser beam as the surface composition detection processes inductor, are the laser induced breakdown spectroscopy (LIBS) and laser induced fluorescence spectroscopy (LIF or LIFS).

Within these two techniques, it is applied laser radiation over a surface producing interaction processes that are monitored, analyzed and interpreted by the means of some dedicated devices and software applications.

At the basis of the LIBS technique stands the production of a plasma plum at the surface of the laser irradiated surface, which emits precise data about the ions found in the composition of the dislocated material, in all directions. This is a micro-destructive technique that provides qualitative and quantitative data over the chemical composition of the sample's surface material. The repeated use of this technique in the same spot, consists a stratigraphic analysis (depth analysis).

LIF technique is similar with the LIBS but has several major differences. It is based on a non-destructive process. It is used a low energy laser beam (preferably UV radiation, because it does not modify the structure or aspect of the irradiated

surface, at the specified parameters) to excite the surface's molecules to induce the fluorescence emission process [3], which is collected afterwards by an optical acquisition device.

Motivation. It is not enough to interrogate single spots in different positions of a surface to gain detailed data about that surface quality. The best way to gather all the data a surface could provide, is to interrogate all of its spots at a high resolution. Therefore there will be needed an automated device that could actually scan a defined area of that surface, spot by spot, based on an mathematical algorithm using an acquisition technique that can provide us with the desired data.

2. SCANNING DEVICE DESCRIPTION

In this paper it is described the structure and the operation setup of such an automated device that facilitates the UV laser induced fluorescence scanning of a defined area and the data acquisition of the emitted fluorescence and the particular case study in an historical parchment.

Point by point laser scanning of an area implies the redirection of the laser beam, emitted by the source 'La', to every spot of that area (respectively with the input resolution) following a predefined algorithm. This device redirects the laser beam with a mirror, mounted on a two stage motors ensemble, controlled by a computer that allows the high precision two central axes rotation of the mirror (0.0005°). The laser beam is transmitted to the redirecting mirror and will be reflected to the sample's surface, interacting with it by inducing the fluorescence emission of the molecules, which will spread in all directions. Some of that emitted fluorescence falls on the redirecting mirror and transmitted through an optical

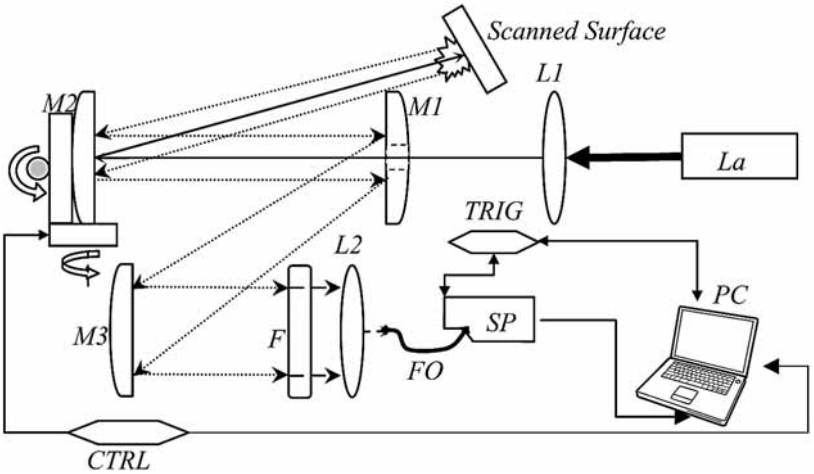

Fig. 1 – Scanning ensemble schematics.

ensemble to a detection device. This optical ensemble, depicted in Fig. 1, is constituted by a perforated mirror 'M1', which allows the laser beam to propagates through its aperture but reflects the fluorescence emission that comes from the redirecting mirror; another redirecting mirror 'M2' that reflects the fluorescence emission through-out an UV filter 'F' (266 nm) up to the optical collector 'L2'; optical fiber 'FO' for optical information transmission between optical collector and the spectrometer 'SP'. It is used a large bandwidth spectrometer to decode/encode optical information into digital data which are processed by a dedicated software on the computer.

2.1. OPTOELECTRONIC SETUP

The irradiation source ***La*** is an active solid state passive Q-switched diode pumped laser that emits at 266 nm with a maximum repetition rate of 3KHz at 1,25 μJ of energy per pulse. The ***L1*** lens focuses the laser beam.

As for detection it was used a low wavelength high sensitive spectrometer, best suited for fluorescence acquisition. It can detect light radiation in the 200-1100 nm bandwidth with a 90% quantum efficiency.

To synchronize the irradiation spot's position changes with the spectra emission acquisition, it was used a device that allows the external software triggering. The ***TRIG*** break-out box is the communication link between the spectrometer and the computer or other triggering devices.

The redirecting mirror's rotational ensemble device is constituted by two stage step motors. These motors can proceed at high precision rotations, with a minimum step of 0.0005° with a maximum speed of 80°/s.

Each motor is connected to a controller ***CTRL*** to communicate with the computer through a serial port. A software application (under the LabView platform) ensures the full control of the motors operation.

The optical collector ***L2*** is a 25.4 mm diameter collimating lens with an open air collimating range of 12 m. This lens transmits the collected data to the spectrometer ***SP*** through the optical fiber ***FO***.

The fluorescent radiation transmission within this device is ensured by the perforated mirror ***M1*** and another redirecting mirror ***M3***.

The whole ensemble is constructed on a solid platform, all the components being arranged and fixed on it as the figure shows. The laser head is mounted on an adjustable platform. ***M1*** and ***M3*** mirrors are mounted on adjustable supports. The optical collector ***L2*** is mounted on an adjustable mini-platform that allows two central axes rotation. In front of the collector it is mounted the UV filter ***F*** to avoid the acquisition of the incident laser beam reflection. The spectrometer ***SP*** is also fixed on the solid platform. The redirecting mirror ***M2*** servo motors ensemble, are mounted on a special structure.

Acquisition timing synchronization with the laser spot repositioning (Fig. 2): the acquisition integration $\boldsymbol{T_I}$ time must be less or equal with the sum of the triggering time $\boldsymbol{T_T}$ together with the waiting time $\boldsymbol{T_A}$ and the motor moving duration time $\boldsymbol{T_P}$. The triggering time represents the duration time of the TTL trigger signal output for the spectrometer, and it is less than 10 ms. The waiting time $\boldsymbol{T_A}$ represents how long the scanning application waits at each step for the acquisition to be done. The motor moving duration time $\boldsymbol{T_P}$ represents the time spent by a motor to move to a new position.

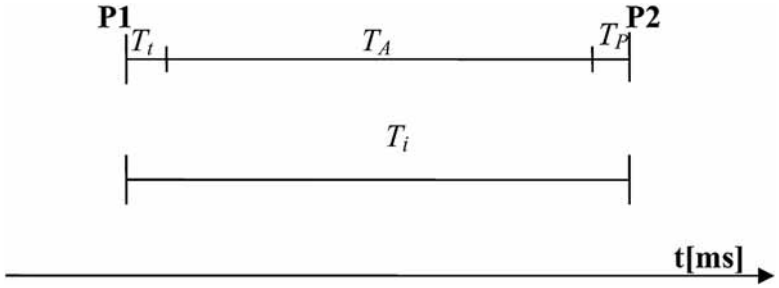

Fig. 2 – Duration timings within a repositioning step: T_t – trigger time; T_p – motor move duration time; T_A – step waiting time; T_i – integration time.

2.2. SOFTWARE ARCHITECTURE

In the following workflow diagram (Fig. 3) is represented the interfacing of the whole scanning system. The instructions within the command blocks have informational role and represents only the major steps within the system workflow. It also depicts the communication channels between the hardware devices and the computer.

The incident laser beam guiding is realized by the two motor mounting which are controlled by a computer software interface. This interface is specially designed to make an easier scanning set up and operation, and communicates with the controllers using the VISA interfacing language on a LabView software support. The scanning algorithm follows the mathematical model for a rectangular matrix crossing pattern for the step by step laser spot repositioning.

The software interface permits the input and modification of all scanning parameters. After inputting the distance between the sample surface and the optical collector, and choosing the desired starting point (the upper left corner of the area) using the direction controls, there must be introduced the vertical and horizontal lengths and the step dimensions to create a matrix model of the area that has to be scanned. Each element of the virtual matrix represents a repositioning step. Each step is calculated depending on the distance $\boldsymbol{D}$ and represents the angular repositioning

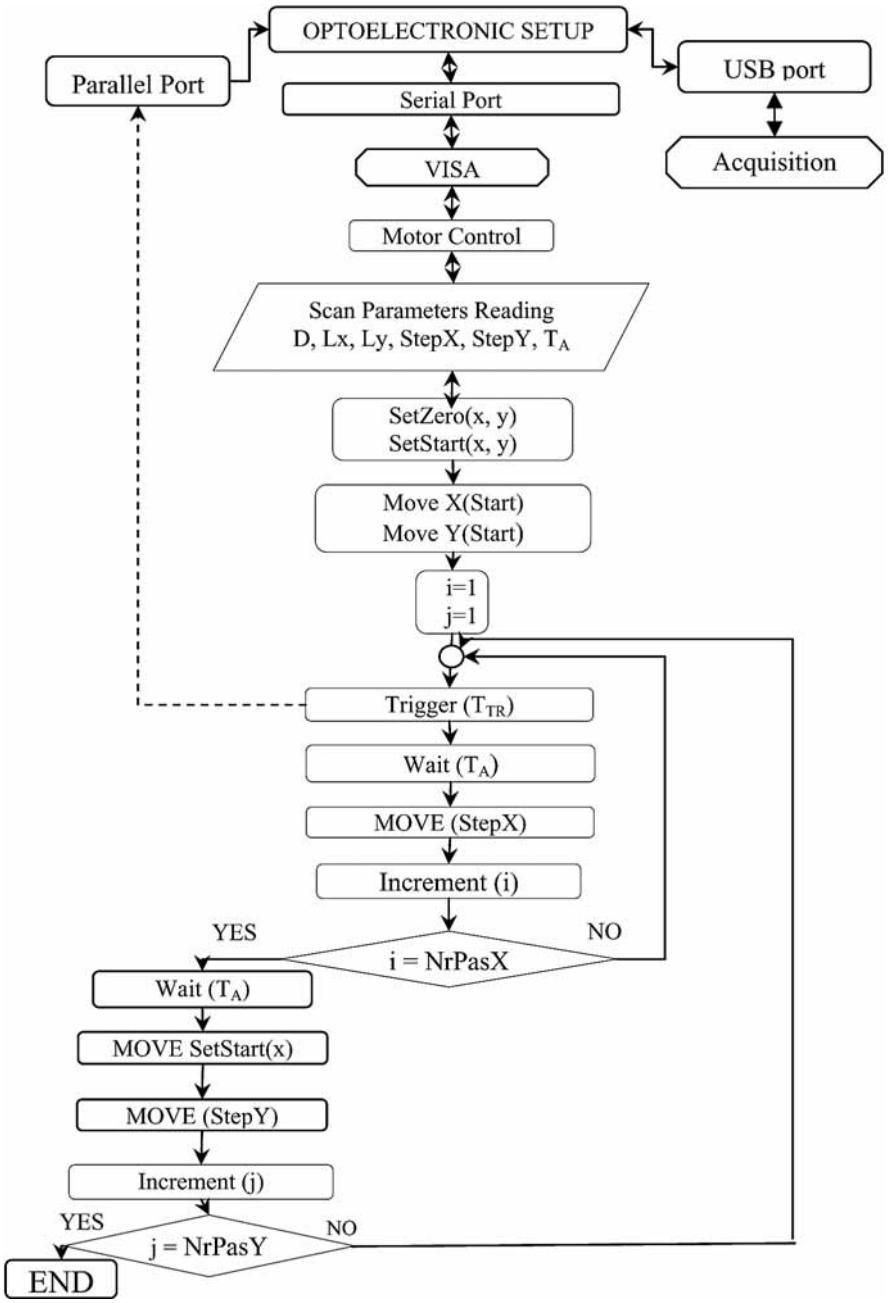

Fig. 3 – Workflow diagram.

repositioning parameter for the motors, so that the laser spot is repositioned at a constant step length. There is another important parameter to be set: the total

waiting time T_A along with the triggering time T_T and the duration time of each motor move T_P must be greater or equal with the integration time T_I set for the acquisition. Usually, the T_A is set at about T_I + 100 ms.

In the acquisition interface it can be set the integration time T_I for a single scan. The Strip Chart option of this application allows the user to set a number of specific bandwidths of interest, reducing considerably the processing time and making the spectra interpretation much easier. A text file for each selected bandwidth is created. The format of these files contains a column with the average intensities of that bandwidth in scanning position.

Another software interface is used for the processing of the resulted data by mapping a replica of the scanned area. This allows the scientist to view the intensity distribution of the desired characteristic fluorescence emissions over the scanned area. This application provides two different viewing modes. The intensity graph mode displays the intensity distribution map of a single channel using a white/blue gradient, with the brightest areas representing the highest fluorescence emission intensity of the selected channel. The RGB replica is also an intensity distribution map, but it allows the selection of three different bandwidths for each R, G and B color channels. The resulted image illustrates a colored intensity distribution map of the scanned area. These images can be saved and used in further discussions, presentations or for documentation.

The main goal of these mapping interpretations is to detect a specific known fluorescence characteristic such as pigments or biological attacks over the artworks surfaces, helping the conservers and artwork restorers to have a better knowledge of the objects surface pigment composition and to prevent the further negative effects of the biological attacks.

3. EXPERIMENTAL

With this experiment it is verified the operation of this device, performing a high resolution scan on an historical parchment, trying to detect the different fluorescence emissions from a selected area.

Using a laser diode that emits in the visibile spectrum, the operator have to adjust the optical collector focus point right on the surface that has to be scanned.

As it can be seen in Fig. 4, a 30×30 mm area of the parchment's surface containing red colored letters, thin red stave lines, and parchment at different degrees of dirt deposition, was selected to be analyzed.

To identify each characteristic spectrum of the different zones of the selected parchment area – as a restorers request – there have been made LIF analysis at different interogation duration times.

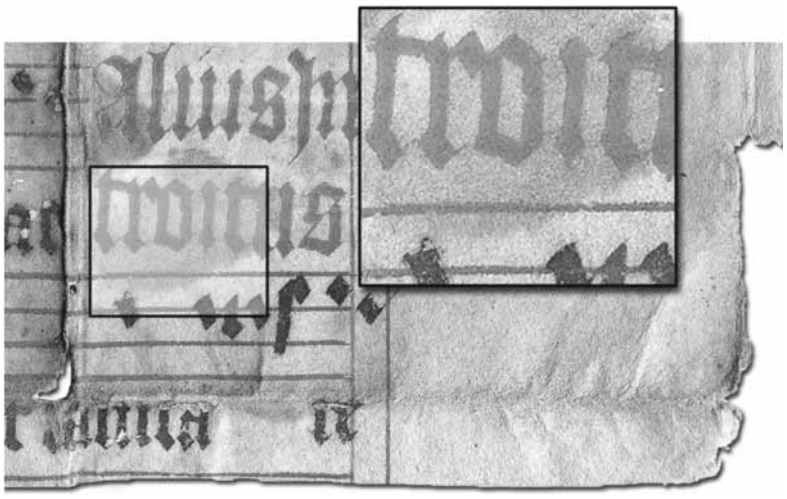

Fig. 4 – Scan area selection.

In the graph below there are represented the most significative areas: the normal and dirty parchment, normal and dirty red pigment and the black colored areas in the bottom of the selection.

It is noticed that the parchment (Fig. 5, solid line) has a high fluorescence emission, even when it is covered with dirt. It is also observed in the red pigment

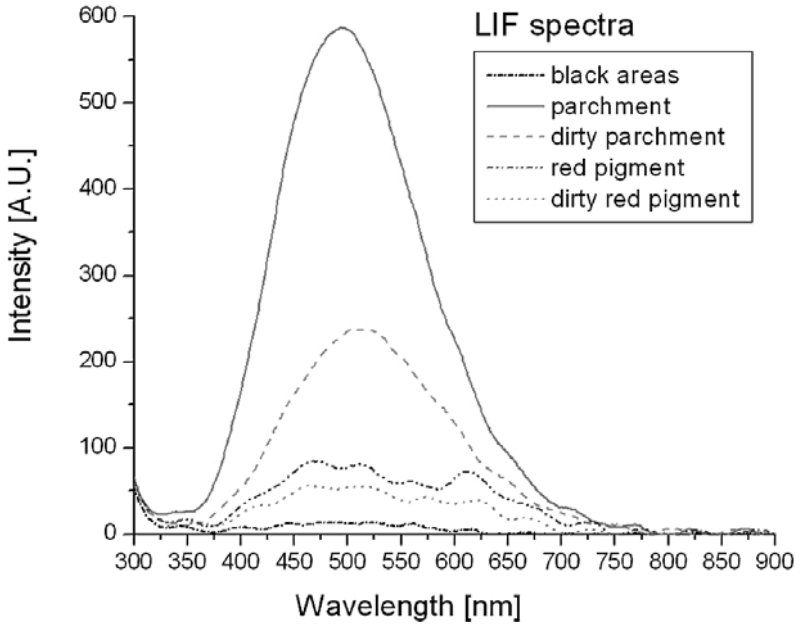

Fig. 5 – LIF spectra of the tested areas.

spectrum that the parchment fluorescence emission has a great influence. The black colored areas (Fig. 5, dash dot line) had absorbed most of the radiation and therefore there was a low fluorescence emission.

To obtain a good spectrum shape the interogation time for the acquisition was set to 1000 ms and 3000 ms (in some cases).

For this particular scan it has been chosen two spectrum characterics: the parchment emission and the red pigment fluorescence emission as follows.

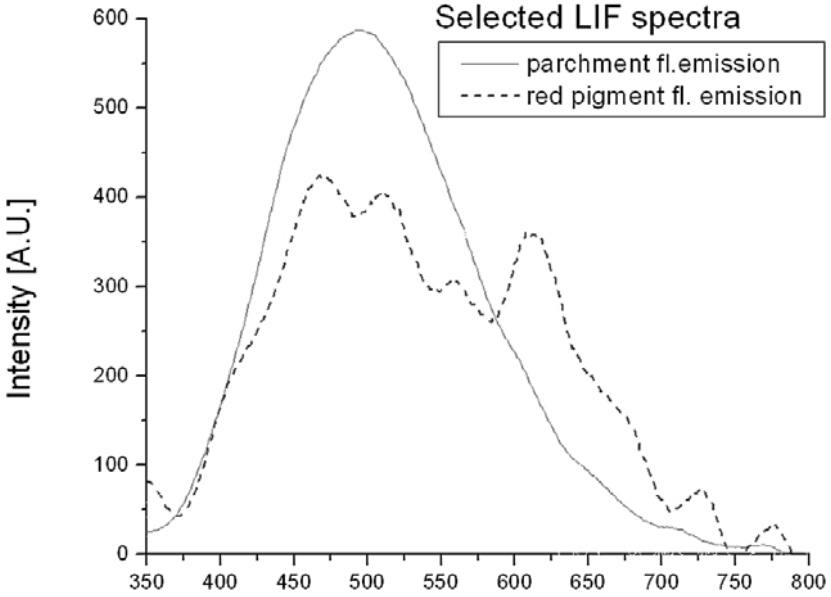

Fig. 6 – The selected emission spectra for the scanning process.

The acquisition aplication was set to record only the average intensity of a 10 nm bandwidth for each of the spectra (525–535 nm for the parchment fluorescence emission spectrum and 601–611 nm for the red pigment fluorescence emission spectrum) to ease the interpretation work.

The scanning resolution was set at 0.2 mm per step (on horizontal and vertical axes) to test the high precision laser spot positioning. This means a total 150×150 points to be interogated. Integration time T_I was set at 350 ms and the T_A time at 450 ms.

After choosing the starting point and with the other scan parameters all set, the scanning process is started and the laser spot is repositioned each time for a new acquisition, following the pattern provided by the programmed algorithm.

At the end of the scan there were obtained two data files containing the average intensities of the selected bandwidths. By merging these two files and using each of bandwidth values as the others one's background it is obtained the

input file for the interpretation software. Using the recorded and corrected data this application rendered the following images:

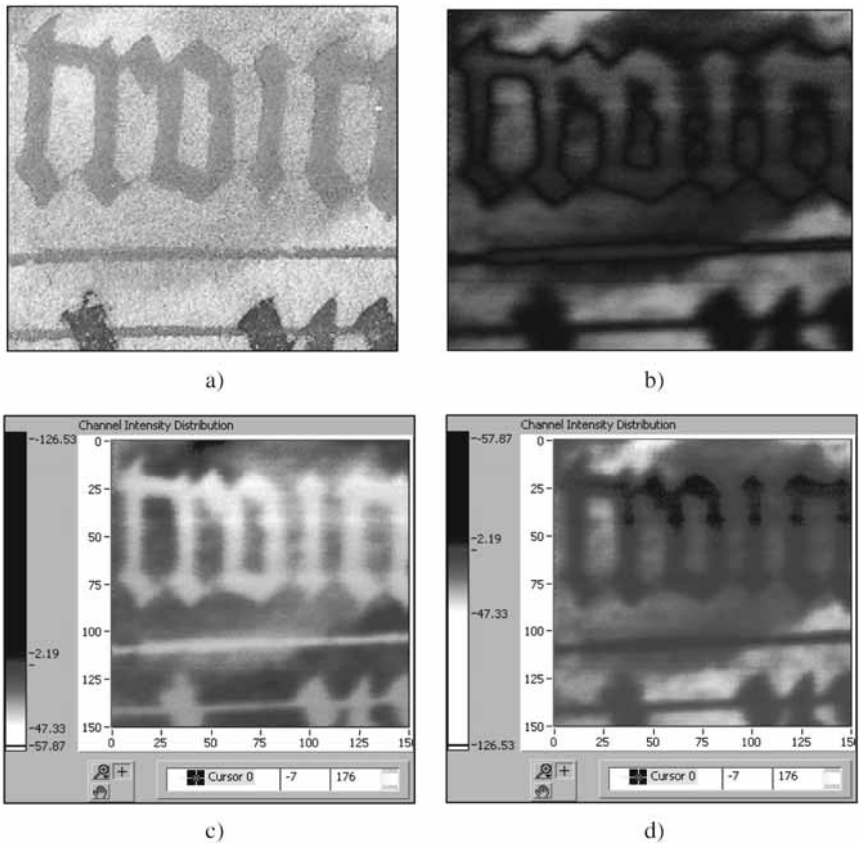

Fig. 7 – Resulted images: a) real image; b) RGB map replica; c) 601–611 nm intensity graph; d) 525–535 nm intensity graph.

4. RESULTS AND DISCUSSION

In the intensity graph view the white/blue/black gradient is used to map the intensity distribution of the selected bandwidth. The brightest areas representing the highest intensity, while the darker areas representing the lowest intensities.

The resulted images, RGB and the intensity distribution maps can be compared with the photo image, here in Fig. 7a.

The RGB color channel view (Fig. 7b) displays a colored combination of the chosen bandwidths by associating to each color channel a single spectrum bandwidth. Here the red pigment fluorescence emission spectrum bandwidth was

associated with the R channel, while the parchment fluorescence emission spectrum bandwidth was associated with the G and B color channels. This colored simulation highlights all the above observations. The stain is clearly delimited from the cleaner parchment area (teal color), as a darker teal color, while the red pigment is represented by the red color. Even the higher fluorescence emission intensity from the top of the letters here is better observed as a brighter red color.

Fig. 7c depicts the 601–611 nm bandwidth intensity distribution map of the emitted fluorescence due to the laser excitation. This represents the red pigment fluorescence emission map. The lowest red pigment fluorescence emission is to be found in the cleaner parchment areas, represented here by the darker blue color. The stain has a higher fluorescence emission intensity in this spectrum bandwidth, therefore it must have a some of the red pigment components. The red letters and the stave lines show the highest fluorescence intensity emission. An interesting fact is that the top of the letters that showed a low fluorescence emission in the parchment spectrum bandwidth, here it displays the highest intensity.

Fig. 7d depicts the 525–535 nm bandwidth intensity distribution map of the emitted fluorescence due to the laser excitation. This represents the parchment fluorescence emission map. The brightest areas show that the cleaner areas of the parchment have a greater fluorescence emission intensity than the dirtier areas. The stained area can be clearly observed as a dark-blue area in the center, similar with the stain in the real image. The pigmented areas (letters, stave lines and black markings) have a lower intensity emission, with the observation that there are some dark areas on the top of the letters that is resulted from a low fluorescence emission in the parchment fluorescence spectrum, therefore there must be a lot of dirt that absorbs most of the laser energy or a much thicker pigment layer than in the rest of the letters.

5. CONCLUSIONS

These results confirms that this automated optoelectronic device can successfully be used for qualitative analysis of artwork objects surfaces helping the art conservers and restorers to easily detect or highlight – in this particular study case – different fluorophore based chemicals or biological attacks. The obtained data provides useful information that can be used in further discussions regarding the conservation steps that should be followed to ensure the safety of the artwork.

In case of a biological attack on the artwork surface, there is no risk of spreading the contamination on the installation hardware or the operator. Being a non-contact technique, it allows complex investigations of fragile and/or very degraded surfaces.

The LIF technique permits repeated analysis of the same spots without affecting the artworks surface due to the low energy radiation used.

This technique finally offers the restorer or conserver in charge the possibility to take better decisions regarding the future steps in any artwork (that can emit

fluorescence) restoration or conservation. The results also consists in a complex proven documentation and a recommended protocol for the valuable objects insurances.

REFERENCES

1. F. Colao, R. Fantoni, L. Fiorani, A. Palucci, I. Gomoiu, *Compact scanning LIDAR fluorosensor for investigations of biodegradation on ancient painted surface,* J. of Opt. and Adv. Materials, **7**, *6*, 3197–3208 (2005).
2. J. Striber, F. Colao, R. Fantoni, L. Fiorani, A. Palucci, *Algorithm for angular correction of images in scanning LIF*, J. of Opt. and Adv. Materials, **9**, *6*, 1918–1925 (2007).
3. J. R. Lakowicz, *Principles of Fluorescence Spectroscopy*, Kluwer Academic, Plenum, New York, 1999.